

Testing NSI suggested by solar neutrino tension in T2HKK and DUNE

Monojit Ghosh^{1,2,3,*} and Osamu Yasuda^{1,†}

¹*Department of Physics, Tokyo Metropolitan University, Hachioji, Tokyo 192-0397, Japan*

²*Department of Physics, School of Engineering Sciences, KTH Royal Institute of Technology, AlbaNova University Center, Roslagstullsbacken 21, SE-106 91 Stockholm, Sweden*

³*The Oskar Klein Centre, AlbaNova University Center, Roslagstullsbacken 21, SE-106 91 Stockholm, Sweden*

Abstract

It was shown that the tension between the mass-squared differences obtained from solar neutrinos and those acquired through KamLAND experiments may be solved by the introduction of a non-standard flavor-dependent interaction (NSI) in neutrino propagation. In this study, we discuss the possibility of testing such a hypothesis using the future long-baseline neutrino experiments T2HKK and DUNE. Assuming that the NSI does not exist, we provide the excluded region within the (ϵ_D, ϵ_N) plane, where ϵ_D and ϵ_N are the parameters appearing in the solar neutrino analysis conducted with the NSI. We find that the best-fit value from the solar neutrino and KamLAND data (global analysis of a particular coupling to quarks) can be tested at more than 10σ (3σ) by these two experiments for most of the parameter space.

* manojit@kth.se

† yasuda@phys.se.tmu.ac.jp

I. INTRODUCTION

It has been well established by solar, atmospheric, reactor and accelerator neutrino experiments that neutrinos have mass and mixings [1]. In the standard three flavor neutrino oscillation framework, there are three mixing angles θ_{12} , θ_{13} , θ_{23} , two mass-squared differences Δm_{31}^2 and Δm_{21}^2 , and one Dirac type CP phase δ_{CP} . The approximate values of the oscillation parameters are determined as follows: $(\Delta m_{21}^2, \sin^2 2\theta_{12}) \simeq (7.5 \times 10^{-5} \text{eV}^2, 0.86)$, $(|\Delta m_{31}^2|, \sin^2 2\theta_{23}) \simeq (2.5 \times 10^{-3} \text{eV}^2, 1.0)$, $\sin^2 2\theta_{13} \simeq 0.09$ [2–4]. Although there are some indications that $\delta_{CP} \sim -90^\circ$ and $\Delta m_{31}^2 > 0$ are favored, we do not know the value of the Dirac CP phase δ_{CP} , the sign of Δm_{31}^2 (the mass hierarchy), or the octant of θ_{23} (the sign of $45^\circ - \theta_{23}$) with a high degree of confidence. To measure these undetermined neutrino oscillation parameters, neutrino oscillation experiments with high statistics, such as T2HK [5], DUNE [6], and T2HKK [7] have been proposed. With these precision measurements, we can also probe the new physics by looking at the deviation from the standard three flavor neutrino mixing scenario.

However, it is well known [8, 9] that tension occurs between the mass-squared difference deduced from the solar neutrino observations and that derived from the KamLAND experiment. While Ref. [8] proposed a sterile neutrino oscillation with a mass-squared difference on the order of $O(10^{-5}) \text{eV}^2$ as a solution of this tension, it was pointed out in Ref. [9] that the tension can be resolved by introducing flavor-dependent non-standard interactions (NSI) in neutrino propagation: [10–12]

$$\mathcal{L}^{\text{NSI}} = -2\sqrt{2}\epsilon_{\alpha\beta}^{ff'P} G_F \bar{\nu}_{\alpha L} \gamma_\mu \nu_{\beta L} \bar{f}_P \gamma^\mu f'_P, \quad (1)$$

where f_P and f'_P are fermions with chirality P , $\epsilon_{\alpha\beta}^{ff'P}$ is a dimensionless constant, and G_F is the Fermi coupling constant. Constraints on $\epsilon_{\alpha\beta}$ have been previously discussed by numerous researchers¹, from atmospheric neutrinos [15–19], e^+e^- colliders [20], the compilation of various neutrino data [21, 22], solar neutrinos [23–25], $\nu_e e$ or $\bar{\nu}_e e$ scatterings [26, 27], solar and reactor neutrinos [28], and solar, reactor, and accelerator neutrinos [29]. The constraints on ϵ_{ee} and $\epsilon_{e\tau}$ from atmospheric neutrino have been discussed in Ref. [30] along with those from long-baseline experiments, in Ref. [31] by the Super-Kamiokande Collaboration, in Refs. [32–36] which discussed future atmospheric neutrino experiments. NSI has recently been studied extensively in terms of long-baseline experiments [37–61]². It is known that some models predict large non-

¹ See Refs. [13, 14] for extensive references.

² Apart from the NSIs occurring during neutrino propagation, NSIs also take place in neutrino production and detection. Such charge current NSIs are more relevant to low-energy experiments [62–64].

standard interactions [65–67], and hence such large NSI effects are worth investigating from the viewpoint of model building.

In the analysis of long-baseline experiments and atmospheric neutrino experiments, the dominant contribution comes from the larger mass squared difference Δm_{31}^2 and the oscillation probabilities are expressed in terms of $\epsilon_{\alpha\beta}$ and the standard oscillation parameters. While the results in Ref. [9] may suggest the existence of NSI, the parametrizations for the NSI parameters (ϵ_D , ϵ_N) in Ref. [9] are different from those with $\epsilon_{\alpha\beta}$, and it remains unclear how the allowed region in Ref. [9] will be tested or excluded through future experiments. In Ref. [68], assuming a standard oscillation scenario, the excluded region within the (ϵ_D , ϵ_N) plane was given for the atmospheric neutrino measurements at Hyper-Kamiokande. In this study, we discuss the sensitivity of the accelerator-based neutrino measurements T2HKK and DUNE to NSIs using the same parametrization as described in Ref. [9]. Because the parametrization used in Ref. [9] differs from $\epsilon_{\alpha\beta}$ on a three flavor basis, a non-trivial mapping is required to compare the results of these two parametrizations.

As with the case of a standard scenario [69–73], parameter degeneracy in the presence of the new physics has also been studied in Refs. [42, 45, 50, 52, 57, 58, 74, 75]. Because little is known regarding parameter degeneracy in the parametrization of ϵ_D and ϵ_N , and because such a study is beyond the scope of this paper, we do not discuss parameter degeneracy herein.

The remainder of this paper is organized as follows. In section II, we describe the neutrino oscillations in the presence of NSIs in neutrino propagation, as well as descriptions of the T2HKK and DUNE experiments. In section III, we describe the correspondence between the parametrization $\epsilon_{\alpha\beta}$ in the long baseline experiments and (ϵ_D , ϵ_N) in the solar neutrino experiments. In section IV, we describe our results. In section V, we draw our concluding remarks.

II. THREE FLAVOR NEUTRINO OSCILLATION FRAMEWORK WITH NSI

A. Nonstandard interactions

The presence of NSIs (Eq. (1)) modifies the neutrino evolution governed by the positive energy part of the Dirac equation:

$$i \frac{d}{dx} \begin{pmatrix} \nu_e(x) \\ \nu_\mu(x) \\ \nu_\tau(x) \end{pmatrix} = \{ U \text{diag}(0, \Delta E_{21}, \Delta E_{31}) U^{-1} + \mathcal{A} \} \begin{pmatrix} \nu_e(x) \\ \nu_\mu(x) \\ \nu_\tau(x) \end{pmatrix}, \quad (2)$$

where U is the leptonic mixing matrix defined by

$$U = \begin{pmatrix} c_{12}c_{13} & s_{12}c_{13} & s_{13}e^{-i\delta_{CP}} \\ -s_{12}c_{23} - c_{12}s_{23}s_{13}e^{i\delta_{CP}} & c_{12}c_{23} - s_{12}s_{23}s_{13}e^{i\delta_{CP}} & s_{23}c_{13} \\ s_{12}s_{23} - c_{12}c_{23}s_{13}e^{i\delta_{CP}} & -c_{12}s_{23} - s_{12}c_{23}s_{13}e^{i\delta_{CP}} & c_{23}c_{13} \end{pmatrix}, \quad (3)$$

and $\Delta E_{jk} \equiv \Delta m_{jk}^2/2E \equiv (m_j^2 - m_k^2)/2E$, $c_{jk} \equiv \cos \theta_{jk}$, and $s_{jk} \equiv \sin \theta_{jk}$. In addition, \mathcal{A} in Eq. (1) indicates the modified matter potential

$$\mathcal{A} \equiv \sqrt{2}G_F N_e \begin{pmatrix} 1 + \epsilon_{ee} & \epsilon_{e\mu} & \epsilon_{e\tau} \\ \epsilon_{\mu e} & \epsilon_{\mu\mu} & \epsilon_{\mu\tau} \\ \epsilon_{\tau e} & \epsilon_{\tau\mu} & \epsilon_{\tau\tau} \end{pmatrix}, \quad (4)$$

$\epsilon_{\alpha\beta}$ is defined by

$$\epsilon_{\alpha\beta} \equiv \sum_{f=e,u,d} \frac{N_f}{N_e} \epsilon_{\alpha\beta}^f, \quad (5)$$

and N_f ($f = e, u, d$) is the number density of fermions f . Here, we define the new NSI parameters as $\epsilon_{\alpha\beta}^{fP} \equiv \epsilon_{\alpha\beta}^{ffP}$ and $\epsilon_{\alpha\beta}^f \equiv \epsilon_{\alpha\beta}^{fL} + \epsilon_{\alpha\beta}^{fR}$ because the matter effect is sensitive only to the coherent scattering and vector part in the interaction. As shown in the definition of $\epsilon_{\alpha\beta}$, the neutrino oscillation experiments conducted on Earth are only sensitive to the sum of $\epsilon_{\alpha\beta}^f$.

B. Solar neutrinos

In Refs. [8, 9] it was pointed out that a tension occurs between the two mass squared differences extracted from the KamLAND and solar neutrino experiments. The mass squared difference Δm_{21}^2

($= 4.7 \times 10^{-5} \text{eV}^2$) extracted from the solar neutrino data is 2σ smaller than that from the KamLAND data Δm_{21}^2 ($= 7.5 \times 10^{-5} \text{eV}^2$). The authors of Refs. [9] indicated that the tension can be removed by introducing an NSI in propagation.

To discuss the effect of the NSI on the solar neutrinos, we reduce the 3×3 Hamiltonian in the Dirac equation, Eq. (2), to an effective 2×2 Hamiltonian to obtain the survival probability $P(\nu_e \rightarrow \nu_e)$ because solar neutrinos are approximately driven by one mass squared difference Δm_{21}^2 [9]. The survival probability $P(\nu_e \rightarrow \nu_e)$ can be written as follows:

$$P(\nu_e \rightarrow \nu_e) = c_{13}^4 P_{\text{eff}} + s_{13}^4. \quad (6)$$

Here, P_{eff} can be calculated using the effective 2×2 Hamiltonian H^{eff} , which is written as

$$H^{\text{eff}} = \frac{\Delta m_{21}^2}{4E} \begin{pmatrix} -\cos 2\theta_{12} & \sin 2\theta_{12} \\ \sin 2\theta_{12} & \cos 2\theta_{12} \end{pmatrix} + \begin{pmatrix} c_{13}^2 A & 0 \\ 0 & 0 \end{pmatrix} + A \sum_{f=e,u,d} \frac{N_f}{N_e} \begin{pmatrix} -\epsilon_D^f & \epsilon_N^f \\ \epsilon_N^{f*} & \epsilon_D^f \end{pmatrix},$$

where ϵ_D^f and ϵ_N^f are linear combinations of the standard NSI parameters:

$$\begin{aligned} \epsilon_D^f &= c_{13}s_{13} \text{Re} [e^{i\delta_{\text{CP}}} (s_{23}\epsilon_{e\mu}^f + c_{23}\epsilon_{e\tau}^f)] - (1 + s_{13}^2) c_{23}s_{23} \text{Re} [\epsilon_{\mu\tau}^f] \\ &\quad - \frac{c_{13}^2}{2} (\epsilon_{ee}^f - \epsilon_{\mu\mu}^f) + \frac{s_{23}^2 - s_{13}^2 c_{23}^2}{2} (\epsilon_{\tau\tau}^f - \epsilon_{\mu\mu}^f) \end{aligned} \quad (7)$$

$$\epsilon_N^f = c_{13} (c_{23}\epsilon_{e\mu}^f - s_{23}\epsilon_{e\tau}^f) + s_{13}e^{-i\delta_{\text{CP}}} [s_{23}^2\epsilon_{\mu\tau}^f - c_{23}^2\epsilon_{\mu\tau}^{f*} + c_{23}s_{23} (\epsilon_{\tau\tau}^f - \epsilon_{\mu\mu}^f)]. \quad (8)$$

Ref. [9] discussed the sensitivity of solar neutrinos and KamLAND experiments to ϵ_D^f and a real ϵ_N^f for either $f = u$ or $f = d$ at a particular time. The best fit values from the solar neutrino and KamLAND data are $(\epsilon_D^u, \epsilon_N^u) = (-0.22, -0.30)$ and $(\epsilon_D^d, \epsilon_N^d) = (-0.12, -0.16)$, whereas those from the global analysis of the neutrino oscillation data are $(\epsilon_D^u, \epsilon_N^u) = (-0.140, -0.030)$ and $(\epsilon_D^d, \epsilon_N^d) = (-0.145, -0.036)$. These results give us a hint regarding the existence of the NSI. In addition to the above, Ref. [9] also discussed the possibility of a dark-side solution ($\Delta m_{21}^2 < 0$ and $\theta_{21} > 45^\circ$), which requires the NSI to be used in the solar neutrino problem. The allowed regions for the dark-side solution are disconnected from those for the standard LMA solution in the $(\epsilon_D^f, \epsilon_N^f)$ plane, whereas those for the dark-side solution within 3σ do not contain the standard scenario $\epsilon_D^f = \epsilon_N^f = 0$.³ Furthermore, in Ref. [78] more general NSI couplings to u and d quarks were considered as follows:

$$\epsilon_{\alpha\beta} = \sqrt{5} (\cos \eta + Y_n \sin \eta) \epsilon_{\alpha\beta}^\eta = \sqrt{5} \frac{\sin(\eta + \eta_0)}{\sin(\eta_0)} \epsilon_{\alpha\beta}^\eta, \quad (9)$$

³ The COHERENT experiment has ruled out the dark-side solution [76]. In Ref. [77], the authors discussed the constraint from the COHERENT data on the NSI.

where $\epsilon_{\alpha\beta}^\eta$ is the overall normalization of the NSI coupling, η is a new parameter used to interpolate $f = u$ ($\eta = \tan^{-1}(1/2) = 26.6^\circ$) and $f = d$ ($\eta = \tan^{-1}(2) = 63.4^\circ$), or $f = p$ ($\eta = 0$) and $f = n$ ($\eta = \pi/2$), and η_0 is defined from the neutron-proton ratio $Y_n \equiv \#(n)/\#(p)$ by $\eta_0 \equiv \tan^{-1}(1/Y_n)$. It was concluded that the point with the best fit in the global analysis is

$$\eta = -\eta_0|_{\text{mantle}} = -\tan^{-1}\left(\frac{1}{Y_n}\right)\Big|_{\text{mantle}} = -\tan^{-1}\left(\frac{1}{1.051}\right) = -43.6^\circ, \quad (10)$$

i.e., as far as the terrestrial experiments are concerned, the scenario without the NSI provides the best fit. In fact, if the condition (10) is satisfied, then the NSI effect disappears in the terrestrial experiments, including T2HKK and DUNE, as discussed below. The condition (10), however, is a certain type of fine tuning, and for a generic value such as $\eta = \tan^{-1}(1/2) = 26.6^\circ$ ($f = u$) or $\eta = \tan^{-1}(2) = 63.4^\circ$ ($f=d$), the NSI effect does not disappear in the terrestrial experiments. Thus, in the following, we adopt $\eta = \tan^{-1}(1/2) = 26.6^\circ$ or $\eta = \tan^{-1}(2) = 63.4^\circ$ as typical reference values for η .

C. T2HKK and DUNE

The T2HKK experiment [7] is a proposal for the future extension of the T2K experiment [79].⁴ Under this proposal, a water Čerenkov detector with a fiducial mass of 187 kt is placed not only in Kamioka (at a baseline length L of 295 km) but also in Korea (at L of $\simeq 1,100$ km); in addition, the power of the beam at J-PARC in Tokai Village is upgraded to 1.3 MW. In a similar manner as the off-axis design (2.5°) used in the T2K experiment, it is assumed that T2HKK uses an off-axis beam at a 1.5° angle between the directions of the decaying charged pions and neutrinos, and the neutrino energy spectrum has a peak at approximately 0.8 GeV.

By contrast, DUNE [6] is another long-baseline experiment planned in the USA. Its baseline length and peak energy are $L=1,300$ km and $E \sim 3$ GeV, respectively. It will be driven by a 1.2 MW proton beam, and is designed to accommodate future beam power upgrades to 2.4 MW. It is expected that a liquid argon detector with a fiducial mass of 40 kt will provide information for a wide range of the neutrino energy.

The matter effect appears in the neutrino oscillation probability, typically in the form of $G_F N_e L / \sqrt{2} = [\rho / (2.6 \text{ g/cm}^3)] [L / (4000 \text{ km})]$. The baseline length of T2HK ($L = 295$ km) is

⁴ The possibility of a second detector in Korea for the T2K experiment was previously discussed [80–95].

too short for the matter effect, and thus T2HK has poor sensitivity to NSIs in the neutrino propagation. The baseline lengths of T2HKK and DUNE are comparable to the typical length, which is estimated based on the matter effect, and thus T2HKK and DUNE are expected to be sensitive to NSIs in the neutrino propagation.

We used GLoBES [96, 97] and MonteCUBES [98] software to simulate all the above experiments described above. The run time of both DUNE and T2HKK are considered to be 10 years. For T2HKK the ratio of neutrino and antineutrino running is 1:3, whereas for DUNE it is 1:1. Our results are consistent with Refs. [6, 7]. We can calculate our sensitivity in terms of χ^2 in the following way:

$$\chi_{\text{stat}}^2 = 2 \sum_i \left\{ \tilde{N}_i^{\text{test}} - N_i^{\text{true}} - N_i^{\text{true}} \log \left(\frac{\tilde{N}_i^{\text{test}}}{N_i^{\text{true}}} \right) \right\}. \quad (11)$$

The index i corresponds to the number of energy bins, and $\tilde{N}_i^{\text{test}}$ indicates the test events obtained through the original test events N_i^{test} by a scale factor used to incorporate the effect of systematic errors in the following manner:

$$\tilde{N}_i^{\text{test}} \equiv \left(1 + \sum_k c_i^k \xi_k \right) N_i^{\text{test}} \quad (12)$$

where c_i^k is the 1σ systematic error corresponding to the pull variable ξ_k , and the index k indicates the number of pull variables. The final χ^2 is obtained by varying ξ_k from -3 to $+3$, corresponding to their 3σ ranges and minimizing the combination of the statistical (χ_{stat}^2) and systematic ($\sum_k \xi_k^2$) contributions over ξ_k as well as the oscillation parameters:

$$\chi^2 = \min_{\xi_k, \text{osc. param}} \left(\chi_{\text{stat}}^2 + \sum_k \xi_k^2 \right). \quad (13)$$

For T2HKK we took an overall systematic error of 3.2% (3.6%) for the appearance (disappearance) channel in neutrino mode and 3.9% (3.6%) for the appearance (disappearance) channel in antineutrino mode. The systematic error is the same for both the signal and background. The systematic error for DUNE is 2% (10%) for the appearance channel and 5% (15%) for the disappearance channel corresponding to the signal (the background). The systematic errors in neutrino and antineutrino mode are the same for DUNE.

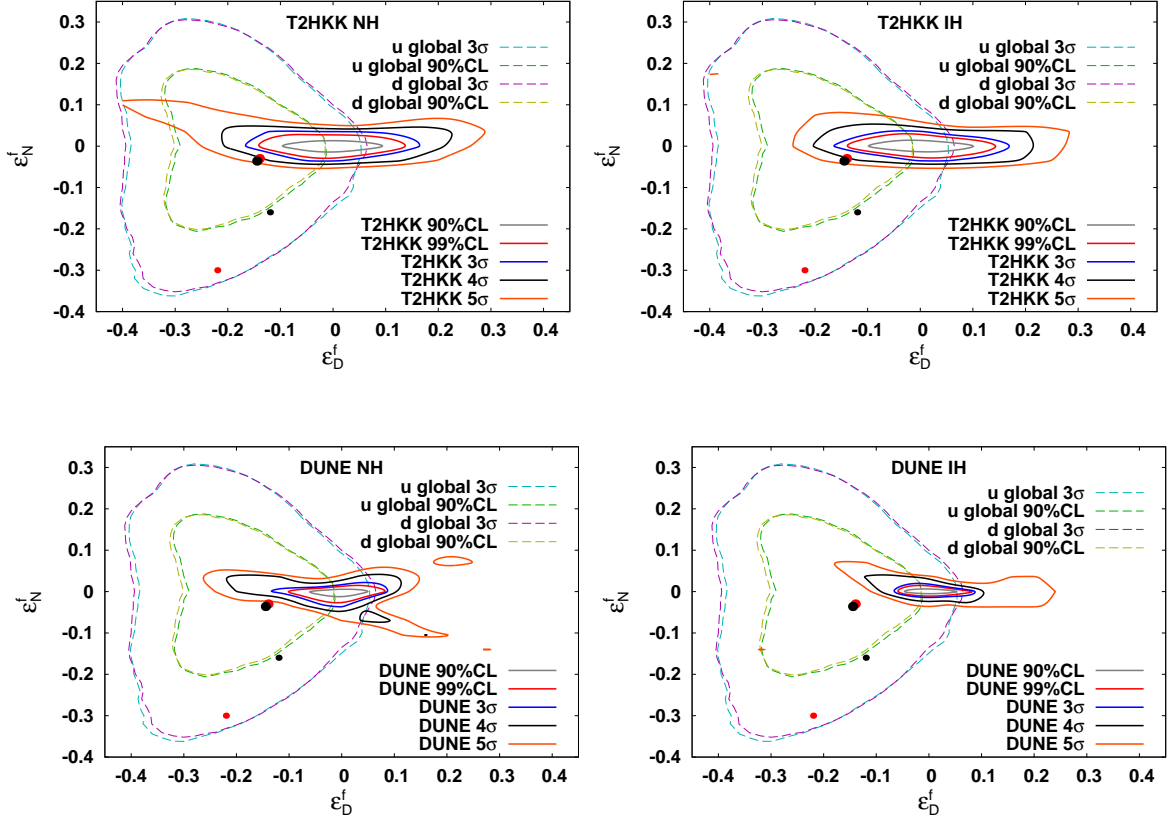


FIG. 1. Excluded regions in (ϵ_D, ϵ_N) plane for T2HKK and DUNE for $\delta_{CP} = -90^\circ$ and $\theta_{23} = 45^\circ$ (outside of the curves). The allowed regions at 90%CL and 3σ suggested by the global analysis [9] are also shown in the dashed curves (inside of the curves). The large (small) red and black circles indicate the best fit points for $f = u$ and $f = d$ from the global (solar + KamLAND) analysis [9], respectively.

III. CORRESPONDENCE BETWEEN THE LONG BASELINE AND SOLAR NEUTRINO EXPERIMENTS

Our strategy applied in this study is to provide the excluded region within the $(\epsilon_D^f, \epsilon_N^f)$ plane by marginalizing all the parameters. This means that, given a set of parameters $(\epsilon_D^f, \epsilon_N^f)$, we have to minimize χ^2 by varying all parameters that satisfy the relations (7) and (8). For this purpose, let us discuss the relation of the NSI parameters $\epsilon_{\alpha\beta}$ to ϵ_D^f and ϵ_N^f . The first thing to note is that the relation between $\epsilon_{\alpha\beta}$ and $(\epsilon_D^f, \epsilon_N^f)$ is a many-to-one mapping, and thus we have to choose the independent and dependent variables from the two relations (7) and (8). In the following, we will treat ϵ_{ee}^f , $|\epsilon_{e\tau}^f|$ and $\epsilon_{\tau\tau}^f$ as dependent parameters and regard all others, namely, θ_{23} , δ_{CP} , $|\epsilon_{e\mu}^f|$,

$\arg(\epsilon_{e\mu}^f)$, $\arg(\epsilon_{e\tau}^f)$, $|\epsilon_{\mu\tau}^f|$, and $\arg(\epsilon_{\mu\tau}^f)$ as independent variables.⁵ The second point to mention is that the constraint on $\epsilon_{\mu\mu}$ is so strong [21, 22] that $|\epsilon_{\mu\mu}|$ is much smaller than the errors of ϵ_{ee}^f and $\epsilon_{\tau\tau}^f$. Thus we can assume that $\epsilon_{\mu\mu} = 0$ has a good approximation in Eqs. (7) and (8). Because the analysis in Ref. [9] was applied for the real ϵ_N^f , Eq. (8) implies that the real part of the right-hand side of Eq. (8) equals ϵ_N^f , whereas the imaginary part of the right-hand side of Eq. (8) disappears. From Eq. (8), we can therefore express $|\epsilon_{e\tau}^f|$ and $\epsilon_{\tau\tau}^f$ in terms of the other parameters as follows:

$$|\epsilon_{e\tau}^f| = \frac{1}{c_{13}c_{23}\sin(\phi_{13} + \delta_{\text{CP}})} (-F \sin \delta_{\text{CP}} + G \cos \delta_{\text{CP}})$$

$$\epsilon_{\tau\tau}^f = \frac{2}{s_{13}\sin 2\theta_{23}\sin(\phi_{13} + \delta_{\text{CP}})} (F \sin \phi_{13} + G \cos \phi_{13})$$

where ϕ_{jk} , F , and G are defined in the following manner:

$$\phi_{12} \equiv \arg(\epsilon_{e\mu}^f), \quad \phi_{13} \equiv \arg(\epsilon_{e\tau}^f), \quad \phi_{23} \equiv \arg(\epsilon_{\mu\tau}^f),$$

$$F \equiv \epsilon_N^f - c_{13}c_{23}|\epsilon_{e\mu}^f| \cos \phi_{12} \tag{14}$$

$$- s_{13}|\epsilon_{\mu\tau}^f| \{ s_{23}^2 \cos(\phi_{23} - \delta_{\text{CP}}) - c_{23}^2 \cos(\phi_{23} + \delta_{\text{CP}}) \}$$

$$G \equiv -c_{13}c_{23}|\epsilon_{e\mu}^f| \sin \phi_{12} \tag{15}$$

$$- s_{13}|\epsilon_{\mu\tau}^f| \{ s_{23}^2 \sin(\phi_{23} - \delta_{\text{CP}}) + c_{23}^2 \sin(\phi_{23} + \delta_{\text{CP}}) \}.$$

After we obtain $|\epsilon_{e\tau}^f|$ and $\epsilon_{\tau\tau}^f$, we obtain ϵ_{ee}^f from Eq. (7):

$$\epsilon_{ee}^f = \frac{2}{c_{13}^2} \left\{ \frac{s_{23}}{2} \sin 2\theta_{13} |\epsilon_{e\mu}^f| \cos(\delta_{\text{CP}} + \phi_{12}) \right.$$

$$+ \frac{c_{23}}{2} \sin 2\theta_{13} |\epsilon_{e\tau}^f| \cos(\delta_{\text{CP}} + \phi_{13})$$

$$- (1 + s_{13}^2) c_{23}s_{23} |\epsilon_{\mu\tau}^f| \cos(\phi_{23})$$

$$\left. - \epsilon_D^f + \frac{s_{23}^2 - s_{13}^2 c_{23}^2}{2} \epsilon_{\tau\tau}^f \right\} \tag{16}$$

Unlike in the case of the solar neutrino analysis with the NSI, in an analysis of the oscillations in the Earth, the ratio of electrons to nucleons $Y_e = \#(p)/(\#(p) + \#(n))$ is approximately 1/2. Thus, we have

$$\epsilon_{\alpha\beta} = 3 \epsilon_{\alpha\beta}^f \tag{17}$$

⁵ The errors of the standard oscillation parameters θ_{12} , Δm_{21}^2 , Δm_{32}^2 , and θ_{13} have little impact on our analysis, and thus we will fix these parameters throughout this study.

ϵ_{ee}	$ \epsilon_{e\tau} $	$\epsilon_{\tau\tau}$	δ_{CP}	θ_{23}	$\arg(\epsilon_{e\tau})$	$ \epsilon_{\mu\tau} $	$\arg(\epsilon_{\mu\tau})$	$ \epsilon_{e\mu} $	$\arg(\epsilon_{e\mu})$	χ^2
0.846	0.123	-0.021	-90	47	0	0	0	0	0	25.46
1.128	0.108	0.511	-90	45	30	0.15	90	0	0	17.54
0.917	0.146	0.114	-90	47	0	0	0	0.03	30	24.61

TABLE I. The values of the oscillation parameters and χ^2 for $(\epsilon_D, \epsilon_N) = (-0.14, -0.03)$ corresponding to T2HKK and NH.

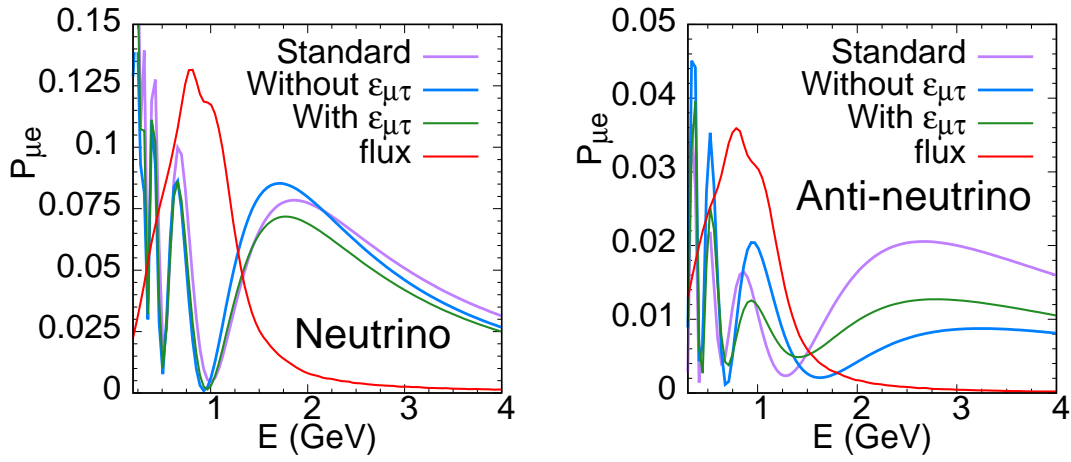


FIG. 2. The appearance probability $P(\nu_\mu \rightarrow \nu_e)$ with and without the NSI parameters. The flux at the detector in Korea is also shown.

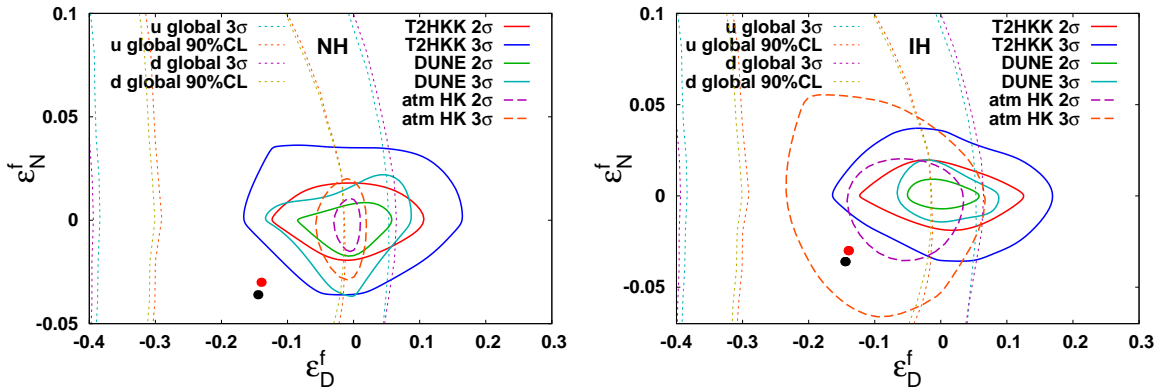


FIG. 3. Comparison of the excluded regions by T2HKK, DUNE, and HK atmospheric neutrino observations [68, 99] in the (ϵ_D, ϵ_N) plane. Others are the same as in Fig. 1.

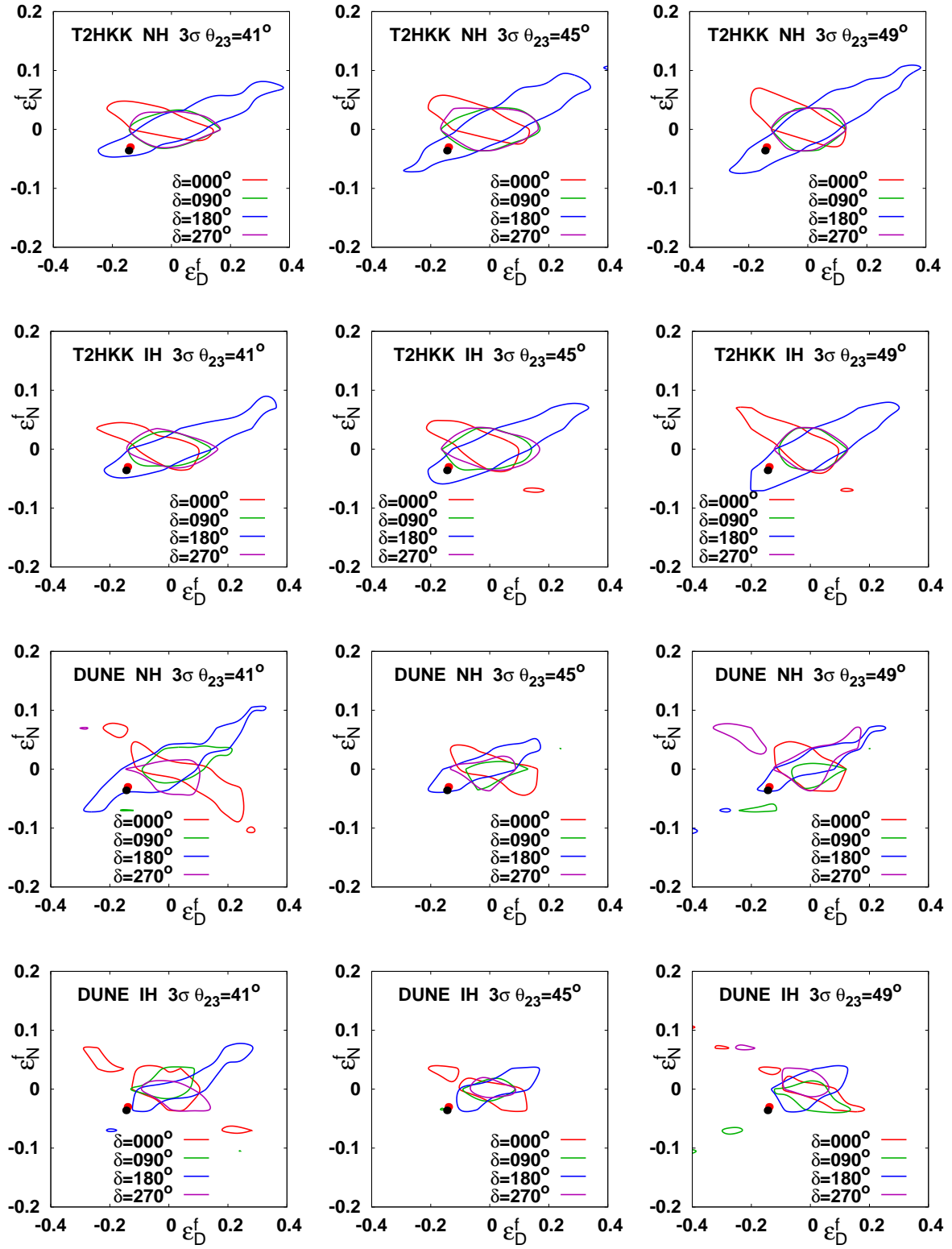


FIG. 4. Dependence of the 3σ excluded region on the true values of δ_{CP} and θ_{23} for T2HKK and DUNE. The red and black circles indicate the best fit points for $f = u$ and $f = d$ from the global analysis [9].

δ_{CP}	θ_{23}	χ^2 (T2HKK)	χ^2 (DUNE)
-180	41	3.45054	5.37943
	45	2.42115	3.74085
	49	4.12396	6.59227
-90	41	18.6853	13.0887
	45	17.5457	31.8923
	49	21.0747	21.2725
0	41	58.7701	26.9004
	45	55.3685	40.5282
	49	53.0394	34.5516
90	41	18.8283	21.0033
	45	11.3261	35.3203
	49	23.2802	9.26665

TABLE II. The values of χ^2 for $(\epsilon_D, \epsilon_N) = (-0.14, -0.03)$ for T2HKK and DUNE in NH.

for either choice of $f = u$ or $f = d$, as can be seen from Eq. (5). In the following, we adopt the parameter $\epsilon_{\alpha\beta}$ which is related to $\epsilon_{\alpha\beta}^f$, using Eq. (17). The constraints on $\epsilon_{\alpha\beta}^f$ for $f = u$ and $f = d$ are given in Ref. [22] for terrestrial experiments, and at 90% CL we have

$$|\epsilon_{e\mu}^f| < 0.05, \quad |\epsilon_{\mu\tau}^f| < 0.05$$

for both $f = u$ and $f = d$. This leads to the following prior on the moduli of $\epsilon_{e\mu} = 3\epsilon_{e\mu}^f$ and $\epsilon_{\mu\tau} = 3\epsilon_{\mu\tau}^f$:

$$\chi_{\text{prior}}^2 = 2.7 \left(\frac{|\epsilon_{e\mu}|}{0.15} \right)^2 + 2.7 \left(\frac{|\epsilon_{\mu\tau}|}{0.15} \right)^2.$$

It is understood that this prior should be included in χ^2 , i.e.,

$$\chi^2 = \min_{\xi_k, \text{osc. param}} \left(\chi_{\text{stat}}^2 + \sum_k \xi_k^2 + \chi_{\text{prior}}^2 \right) \quad (18)$$

In our analysis we found that the effects of $|\epsilon_{e\mu}^f|$ and $\arg(\epsilon_{e\mu}^f)$ are small compared to those of $|\epsilon_{\mu\tau}|$ and $\arg(\epsilon_{\mu\tau})$. In the following analysis, we therefore fix the value of $|\epsilon_{e\mu}^f|$ to zero, which we discuss in detail in the next section.

IV. RESULTS

Assuming that nature is described by standard oscillation scheme and that the mass hierarchy is known, we can obtain χ^2 at each point in the $(\epsilon_D^f, \epsilon_N^f)$ plane for T2HKK and DUNE. The excluded regions at 90%CL, 99%CL, 3σ , 4σ , and 5σ are shown in Fig. 1. The true oscillation parameters are $\sin^2 2\theta_{12} = 0.84$, $\Delta m_{21}^2 = 7.8 \times 10^{-5} \text{eV}^2$, $\Delta m_{31}^2 = 2.5 \times 10^{-3} \text{eV}^2$, $\theta_{23} = 45^\circ$, $\sin^2 2\theta_{13} = 0.09$, and $\delta_{CP} = -90^\circ$. For comparison, the allowed regions at 90%CL and 3σ suggested by the global analysis in Ref. [9] are also depicted. The large (small) red and black circles indicate the best fit points for $f = u$ and $f = d$ from the global (solar + KamLAND) analysis, respectively. The left column is for a normal hierarchy ($\Delta m_{31}^2 > 0$: NH) and the right column is for an inverted hierarchy ($\Delta m_{31}^2 < 0$: IH), whereas the first row is for T2HKK and the second row is for DUNE.

In general, the sensitivity of DUNE is better than that of T2HKK. We can see that both experiments will exclude some of the regions suggested by the global analysis, although it is difficult for both experiments to exclude the region near the origin (the standard scenario). The best-fit point of the combined analysis of the solar neutrino and KamLAND data by Ref. [9] can be excluded at more than 10σ , whereas the best fit point of the global analysis in Ref. [9] can be excluded at 3σ , by both T2HKK and DUNE. For T2HKK the sensitivity is same for both NH and IH, whereas for DUNE the sensitivity in IH is slightly better than NH. It is remarkable that the excluded region is relatively horizontal, i.e., the constraint is stronger in the direction of ϵ_N^f compared to the one of ϵ_D^f . This is because the appearance probability $P(\nu_\mu \rightarrow \nu_e)$ is sensitive to $|\epsilon_{e\tau}| \sim |\epsilon_N^f|$ whereas $\epsilon_D^f \sim \epsilon_{ee}$ changes the magnitude of the matter effect, and the accelerator-based long baseline experiments with energy $E_\nu \sim$ of a few GeV and baseline lengths $L \sim (1000\text{km})$ are not very sensitive to the matter effect.

Now let us discuss the effects of $\epsilon_{e\mu}$ and $\epsilon_{\mu\tau}$. To understand these, we calculate χ^2 for the NSI parameter set $(\epsilon_D, \epsilon_N) = (-0.14, -0.03)$, which is the best fit point of the global analysis for $f = u$ in Ref. [9], for three cases: (i) $|\epsilon_{e\mu}| = 0$ and $|\epsilon_{\mu\tau}| = 0$, (ii) $|\epsilon_{e\mu}| = 0$ and $|\epsilon_{\mu\tau}| \neq 0$, and (iii) $|\epsilon_{e\mu}| \neq 0$ and $|\epsilon_{\mu\tau}| = 0$. We do this for T2HKK and NH. The value of χ^2 for these three cases is 25.46, 17.54 and 24.61, respectively. From these, it is clear that we have a greater effect from $\epsilon_{\mu\tau}$ on the sensitivity than that from $\epsilon_{e\mu}$. We list the values of the different oscillation parameters corresponding to χ^2 , as mentioned above in Table I. To understand this further, in Fig. 2 we plotted the appearance channel probability versus energy for the T2HKK baseline for cases (ii) and (iii) along with the standard, i.e., without the NSI. The values of θ_{23} and δ_{CP} are 45°

and -90° , respectively. The left panel is for neutrinos and the right panel is for antineutrino. In the panels, we also show the corresponding fluxes (in arbitrary units). From the panels, we can see that within the energy range $E < 2$ GeV (which is the region of interest for T2HKK) the separation between the standard and green curves is less conspicuous than the separation between the standard and purple curves. This explains why introducing $\epsilon_{\mu\tau}$ affects the sensitivity in a more significant way than introducing $\epsilon_{e\mu}$.

For comparison with the HK atmospheric neutrino observation, which is analyzed in Refs. [68] and [99], in Fig. 3 we show the excluded regions at 2σ and 3σ for T2HKK, DUNE and HK atmospheric neutrino observations. The analysis of the HK atmospheric neutrino observation in Refs. [68] and [99] was performed using codes that were applied in Ref. [100–103] under the assumption that the HK fiducial volumes are 0.56 Mton, which is the old design of HK, and that the observation is conducted for 12 years, that the HK detector has the same detection efficiencies as those of Super-Kamiokande (SK), and the HK atmospheric neutrino data comprise the sub-GeV, multi-GeV and upward going μ events as in the case of SK. In the case of a normal hierarchy, we can see from Fig. 3 that the sensitivity of the HK atmospheric neutrino experiment is better than that of the accelerator-based experiments, particularly with respect to ϵ_D . This is because the atmospheric neutrino experiment has information from a wide range of baseline lengths up to the diameter of the Earth ($\sim 13000\text{km}$) and it is more sensitive to the matter effect. By contrast, in the case of an inverted hierarchy, the sensitivity of the HK atmospheric neutrino experiment is inferior. This is because atmospheric neutrino experiments with water Čerenkov detectors cannot distinguish neutrinos from antineutrinos and measure only the sum of neutrinos and antineutrinos. This leads to a destructive phenomenon in which the deviations of the neutrino and antineutrino modes are averaged out [103]. In the case of accelerator-based experiments, which separately measure the neutrino and antineutrino modes, such a destructive phenomenon does not occur and the sensitivity for an inverted hierarchy is almost the same as that for a normal hierarchy.

In Figs. 1 - 3 we assume that the true oscillation parameters are $\theta_{23} = 45^\circ$ and $\delta_{CP} = -90^\circ$. We also studied the dependence of the excluded regions on the true oscillation parameters θ_{23} and δ_{CP} , and the results are given in Fig. 4. The first two rows are for T2HKK, whereas the third and fourth rows correspond to DUNE. Each panel of Fig. 4 corresponds to a particular true value of θ_{23} , and the four contours correspond to four different values of δ_{CP} . We considered three choices of a true θ_{23} , which are 41° , 45° and 49° along with four choices of δ_{CP} , which are 0° , 90° , 180° , 270° . In these plots, the red and black circles are the best fit points for $f = u$ and $f = d$ from the global

analysis, respectively. From these plots the following features can be observed:

- The dependence of the excluded regions on θ_{23} is small, whereas the dependence on δ_{CP} is relatively large.
- The sensitivity of T2HKK for NH and IH is almost same whereas for DUNE the sensitivities are different in NH and IH. In fact for DUNE, the sensitivity in IH is slightly better than NH. This can be attributed to the fact that for T2HKK we have taken a 1:3 running of neutrino and antineutrino beam, whereas for DUNE this ratio is 1:1.
- In T2HKK the sensitivities corresponding to $\delta_{CP} = 90^\circ$ and 270° are almost same, but this is not the case for DUNE, which may be due to the fact that T2HKK will use a narrow band flux and mainly covers the second oscillation maximum, whereas for DUNE the flux is wide band and it covers both the first and second oscillation maximum.
- Among the four choices of δ_{CP} , the sensitivity is poor for $\delta_{CP} = 180^\circ$. This is true for both T2HKK and DUNE.
- The best-fit points can be ruled out at 3σ for all combinations of θ_{23} and δ_{CP} in T2HKK and (DUNE, NH) except for, $\delta_{CP} = 180^\circ$. For (DUNE, IH), even the best-fit points for $\delta_{CP} = 180^\circ$ can be excluded at 3σ .

Finally in Table II, we give χ^2 for the best-fit point $(\epsilon_D, \epsilon_N) = (-0.14, -0.03)$ in NH. The numbers in the table also confirm that the capability of T2HKK and DUNE to exclude the NSI best fit point does not depend much on the true value of θ_{23} but does heavily depend upon the true value of δ_{CP} . The sensitivity is at maximum for $\delta_{CP} = 0^\circ$ and is worst for $\delta_{CP} = 180^\circ$ in NH. From the table, we can also understand that the capability of T2HKK to exclude this particular best-fit point is better than DUNE for $\delta_{CP} = 0^\circ$, $(\delta_{CP} = 90^\circ, \theta_{23} = 49^\circ)$, and $(\delta_{CP} = -90^\circ, \theta_{23} = 41^\circ)$.

V. CONCLUSION

In this study, we considered the sensitivity of the future accelerator-based neutrino long-baseline experiments T2HKK and DUNE to the NSI, which was suggested based on the tension between the mass squared differences from the solar neutrinos and KamLAND data. We provided the excluded regions in the (ϵ_D, ϵ_N) plane, and it turns out that the sensitivity of DUNE is slightly

better than that of T2HKK. We found that the both experiments will exclude some of the regions suggested by the global analysis for $f = u$ and $f = d$, although it is difficult for both experiments to exclude the region near the standard scenario point. If there are no non-standard interactions in nature, then the best-fit point of the combined analysis of the solar neutrino and KamLAND data by Ref. [9] can be excluded at more than 10σ for $f = u$ and $f = d$, whereas the best fit point of the global analysis for $f = u$ and $f = d$ in Ref. [9] can be excluded at 3σ by T2HKK and DUNE for most of the parameter space. Although we have discussed only the two cases of $f = u$ and $f = d$, we expect that the sensitivity of T2HKK and DUNE to the NSI parameters (ϵ_N in particular) is better than the existing experiments for wide range of η because the χ^2 distribution is smooth between $\eta = 26.6^\circ$ and $\eta = 63.4^\circ$ on the left panel of Fig.4 of Ref. [78], and the allowed region is expected to more or less similar to the one which we obtain in this work. However, if the NSI exists and the NSI parameter η happens to be close to $\eta_0 = -43.6^\circ$, then both T2HKK and DUNE will have no sensitivity to the NSI. In this case, however, T2HKK and DUNE are expected to give stronger bound on the deviation $|\eta - \eta_0|$ because the allowed region by T2HKK and DUNE in our analysis for $f = u$ and $f = d$ is smaller than that allowed by the existing experiments. We found that accelerator-based long baseline experiments are more sensitive to the parameter ϵ_N than to ϵ_D . The sensitivity of the two experiments were demonstrated to be comparable to, or in the case of an inverted hierarchy, even better than that of the HK atmospheric neutrino experiment.

If the tension between the solar and KamLAND experiments is due to the NSI in neutrino propagation and if the true values of the parameters lie near the best fit point for $f = u$ or $f = d$, we may be able to see an affirmative signal in these long baseline experiments in the future.

ACKNOWLEDGMENTS

The authors would like to thank Shinya Fukasawa for his help with the atmospheric neutrino code. This research was partly supported by a Grant-in-Aid for Scientific Research of the Ministry of Education, Science and Culture, under Grant Nos. 25105009, 15K05058, 25105001, and 15K21734.

[1] C. Patrignani *et al.* (Particle Data Group), [Chin. Phys. C40, 100001 \(2016\)](#).

- [2] F. Capozzi, E. Di Valentino, E. Lisi, A. Marrone, A. Melchiorri, and A. Palazzo, *Phys. Rev.* **D95**, 096014 (2017), [arXiv:1703.04471 \[hep-ph\]](#).
- [3] P. F. de Salas, D. V. Forero, C. A. Ternes, M. Tortola, and J. W. F. Valle, (2017), [arXiv:1708.01186 \[hep-ph\]](#).
- [4] I. Esteban, M. C. Gonzalez-Garcia, M. Maltoni, I. Martinez-Soler, and T. Schwetz, *JHEP* **01**, 087 (2017), [arXiv:1611.01514 \[hep-ph\]](#).
- [5] K. Abe *et al.*, (2011), [arXiv:1109.3262 \[hep-ex\]](#).
- [6] R. Acciarri *et al.* (DUNE), (2015), [arXiv:1512.06148 \[physics.ins-det\]](#).
- [7] K. Abe *et al.* (Hyper-Kamiokande proto-), (2016), [arXiv:1611.06118 \[hep-ex\]](#).
- [8] P. C. de Holanda and A. Yu. Smirnov, *Phys. Rev.* **D83**, 113011 (2011), [arXiv:1012.5627 \[hep-ph\]](#).
- [9] M. C. Gonzalez-Garcia and M. Maltoni, *JHEP* **09**, 152 (2013), [arXiv:1307.3092 \[hep-ph\]](#).
- [10] L. Wolfenstein, *Phys. Rev.* **D17**, 2369 (1978).
- [11] M. M. Guzzo, A. Masiero, and S. T. Petcov, *Phys. Lett.* **B260**, 154 (1991).
- [12] E. Roulet, *Phys. Rev.* **D44**, 935 (1991).
- [13] T. Ohlsson, *Rept. Prog. Phys.* **76**, 044201 (2013), [arXiv:1209.2710 \[hep-ph\]](#).
- [14] O. G. Miranda and H. Nunokawa, *New J. Phys.* **17**, 095002 (2015), [arXiv:1505.06254 \[hep-ph\]](#).
- [15] M. C. Gonzalez-Garcia, M. M. Guzzo, P. I. Krastev, H. Nunokawa, O. L. G. Peres, V. Pleitez, J. W. F. Valle, and R. Zukanovich Funchal, *Phys. Rev. Lett.* **82**, 3202 (1999), [arXiv:hep-ph/9809531 \[hep-ph\]](#).
- [16] P. Lipari and M. Lusignoli, *Phys. Rev.* **D60**, 013003 (1999), [arXiv:hep-ph/9901350 \[hep-ph\]](#).
- [17] N. Fornengo, M. C. Gonzalez-Garcia, and J. W. F. Valle, *JHEP* **07**, 006 (2000), [hep-ph/9906539](#).
- [18] N. Fornengo, M. Maltoni, R. T. Bayo, and J. W. F. Valle, *Phys. Rev.* **D65**, 013010 (2001), [hep-ph/0108043](#).
- [19] M. C. Gonzalez-Garcia and M. Maltoni, *Phys. Rev.* **D70**, 033010 (2004), [arXiv:hep-ph/0404085 \[hep-ph\]](#).
- [20] Z. Berezhiani and A. Rossi, *Phys. Lett.* **B535**, 207 (2002), [hep-ph/0111137](#).
- [21] S. Davidson, C. Pena-Garay, N. Rius, and A. Santamaria, *JHEP* **03**, 011 (2003), [arXiv:0302093 \[hep-ph\]](#).
- [22] C. Biggio, M. Blennow, and E. Fernandez-Martinez, *JHEP* **08**, 090 (2009), [arXiv:0907.0097 \[hep-ph\]](#).
- [23] A. Friedland, C. Lunardini, and C. Pena-Garay, *Phys. Lett.* **B594**, 347 (2004), [hep-ph/0402266](#).

- [24] O. G. Miranda, M. A. Tortola, and J. W. F. Valle, *JHEP* **10**, 008 (2006), [arXiv:hep-ph/0406280](#).
- [25] A. Palazzo and J. W. F. Valle, *Phys. Rev.* **D80**, 091301 (2009), [arXiv:0909.1535 \[hep-ph\]](#).
- [26] J. Barranco, O. G. Miranda, C. A. Moura, and J. W. F. Valle, *Phys. Rev.* **D73**, 113001 (2006), [hep-ph/0512195](#).
- [27] J. Barranco, O. G. Miranda, C. A. Moura, and J. W. F. Valle, (2007), [arXiv:0711.0698 \[hep-ph\]](#).
- [28] A. Bolanos, O. G. Miranda, A. Palazzo, M. A. Tortola, and J. W. F. Valle, *Phys. Rev.* **D79**, 113012 (2009), [arXiv:0812.4417 \[hep-ph\]](#).
- [29] F. J. Escrivuela, O. G. Miranda, M. A. Tortola, and J. W. F. Valle, *Phys. Rev.* **D80**, 105009 (2009), [Erratum: *Phys. Rev.* **D80**, 129908(2009)], [arXiv:0907.2630 \[hep-ph\]](#).
- [30] M. C. Gonzalez-Garcia, M. Maltoni, and J. Salvado, *JHEP* **05**, 075 (2011), [arXiv:1103.4365 \[hep-ph\]](#).
- [31] G. Mitsuka *et al.* (Super-Kamiokande), *Phys. Rev.* **D84**, 113008 (2011), [arXiv:1109.1889 \[hep-ex\]](#).
- [32] T. Ohlsson, H. Zhang, and S. Zhou, *Phys. Rev.* **D88**, 013001 (2013), [arXiv:1303.6130 \[hep-ph\]](#).
- [33] A. Esmaili and A. Yu. Smirnov, *JHEP* **06**, 026 (2013), [arXiv:1304.1042 \[hep-ph\]](#).
- [34] A. Chatterjee, P. Mehta, D. Choudhury, and R. Gandhi, *Phys. Rev.* **D93**, 093017 (2016), [arXiv:1409.8472 \[hep-ph\]](#).
- [35] S. Choubey and T. Ohlsson, *Phys. Lett.* **B739**, 357 (2014), [arXiv:1410.0410 \[hep-ph\]](#).
- [36] S. Choubey, A. Ghosh, T. Ohlsson, and D. Tiwari, *JHEP* **12**, 126 (2015), [arXiv:1507.02211 \[hep-ph\]](#).
- [37] A. Friedland and I. M. Shoemaker, (2012), [arXiv:1207.6642 \[hep-ph\]](#).
- [38] R. Adhikari, S. Chakraborty, A. Dasgupta, and S. Roy, *Phys. Rev.* **D86**, 073010 (2012), [arXiv:1201.3047 \[hep-ph\]](#).
- [39] M. Masud, A. Chatterjee, and P. Mehta, *J. Phys.* **G43**, 095005 (2016), [arXiv:1510.08261 \[hep-ph\]](#).
- [40] A. de Gouvêa and K. J. Kelly, *Nucl. Phys.* **B908**, 318 (2016), [arXiv:1511.05562 \[hep-ph\]](#).
- [41] Z. Rahman, A. Dasgupta, and R. Adhikari, *J. Phys.* **G42**, 065001 (2015), [arXiv:1503.03248 \[hep-ph\]](#).
- [42] P. Coloma, *JHEP* **03**, 016 (2016), [arXiv:1511.06357 \[hep-ph\]](#).
- [43] J. Liao, D. Marfatia, and K. Whisnant, *Phys. Rev.* **D93**, 093016 (2016), [arXiv:1601.00927 \[hep-ph\]](#).
- [44] C. Soumya and R. Mohanta, *Phys. Rev.* **D94**, 053008 (2016), [arXiv:1603.02184 \[hep-ph\]](#).
- [45] M. Blennow, S. Choubey, T. Ohlsson, D. Pramanik, and S. K. Raut, *JHEP* **08**, 090 (2016), [arXiv:1606.08851 \[hep-ph\]](#).

- [46] D. V. Forero and P. Huber, [Phys. Rev. Lett. **117**, 031801 \(2016\)](#), [arXiv:1601.03736 \[hep-ph\]](#).
- [47] K. Huitu, T. J. Krkkinen, J. Maalampi, and S. Vihonen, [Phys. Rev. **D93**, 053016 \(2016\)](#), [arXiv:1601.07730 \[hep-ph\]](#).
- [48] P. Bakhti and Y. Farzan, [JHEP **07**, 109 \(2016\)](#), [arXiv:1602.07099 \[hep-ph\]](#).
- [49] M. Masud and P. Mehta, [Phys. Rev. **D94**, 013014 \(2016\)](#), [arXiv:1603.01380 \[hep-ph\]](#).
- [50] P. Coloma and T. Schwetz, [Phys. Rev. **D94**, 055005 \(2016\)](#), [arXiv:1604.05772 \[hep-ph\]](#).
- [51] M. Masud and P. Mehta, [Phys. Rev. **D94**, 053007 \(2016\)](#), [arXiv:1606.05662 \[hep-ph\]](#).
- [52] S. K. Agarwalla, S. S. Chatterjee, and A. Palazzo, [Phys. Lett. **B762**, 64 \(2016\)](#), [arXiv:1607.01745 \[hep-ph\]](#).
- [53] S.-F. Ge and A. Yu. Smirnov, [JHEP **10**, 138 \(2016\)](#), [arXiv:1607.08513 \[hep-ph\]](#).
- [54] J. Liao, D. Marfatia, and K. Whisnant, (2016), [arXiv:1609.01786 \[hep-ph\]](#).
- [55] S. Fukasawa, M. Ghosh, and O. Yasuda, (2016), [arXiv:1609.04204 \[hep-ph\]](#).
- [56] M. Blennow, P. Coloma, E. Fernandez-Martinez, J. Hernandez-Garcia, and J. Lopez-Pavon, (2016), [arXiv:1609.08637 \[hep-ph\]](#).
- [57] J. Liao, D. Marfatia, and K. Whisnant, [JHEP **01**, 071 \(2017\)](#), [arXiv:1612.01443 \[hep-ph\]](#).
- [58] K. N. Deepthi, S. Goswami, and N. Nath, (2016), [arXiv:1612.00784 \[hep-ph\]](#).
- [59] S. Fukasawa, M. Ghosh, and O. Yasuda, [Phys. Rev. **D95**, 055005 \(2017\)](#), [arXiv:1611.06141 \[hep-ph\]](#).
- [60] M. Ghosh and O. Yasuda, [Phys. Rev. **D96**, 013001 \(2017\)](#), [arXiv:1702.06482 \[hep-ph\]](#).
- [61] M. Masud, M. Bishai, and P. Mehta, (2017), [arXiv:1704.08650 \[hep-ph\]](#).
- [62] A. N. Khan, [Phys. Rev. **D93**, 093019 \(2016\)](#), [arXiv:1605.09284 \[hep-ph\]](#).
- [63] A. N. Khan and D. W. McKay, [JHEP **07**, 143 \(2017\)](#), [arXiv:1704.06222 \[hep-ph\]](#).
- [64] J. Tang and Y. Zhang, (2017), [arXiv:1705.09500 \[hep-ph\]](#).
- [65] Y. Farzan, [Phys. Lett. **B748**, 311 \(2015\)](#), [arXiv:1505.06906 \[hep-ph\]](#).
- [66] Y. Farzan and J. Heeck, [Phys. Rev. **D94**, 053010 \(2016\)](#), [arXiv:1607.07616 \[hep-ph\]](#).
- [67] Y. Farzan, in *18th International Workshop on Neutrino Factories and Future Neutrino Facilities Search (NuFact16)* [Q](#) (2016) [arXiv:1612.04971 \[hep-ph\]](#).
- [68] S. Fukasawa and O. Yasuda, [Nucl. Phys. **B914**, 99 \(2017\)](#), [arXiv:1608.05897 \[hep-ph\]](#).
- [69] J. Burguet-Castell, M. B. Gavela, J. J. Gomez-Cadenas, P. Hernandez, and O. Mena, [Nucl. Phys. **B608**, 301 \(2001\)](#), [arXiv:hep-ph/0103258 \[hep-ph\]](#).
- [70] H. Minakata and H. Nunokawa, [JHEP **10**, 001 \(2001\)](#), [arXiv:hep-ph/0108085 \[hep-ph\]](#).

- [71] G. L. Fogli and E. Lisi, *Phys. Rev.* **D54**, 3667 (1996), [arXiv:hep-ph/9604415 \[hep-ph\]](#).
- [72] V. Barger, D. Marfatia, and K. Whisnant, *Phys. Rev.* **D65**, 073023 (2002), [arXiv:hep-ph/0112119 \[hep-ph\]](#).
- [73] M. Ghosh, P. Ghoshal, S. Goswami, N. Nath, and S. K. Raut, *Phys. Rev.* **D93**, 013013 (2016), [arXiv:1504.06283 \[hep-ph\]](#).
- [74] P. Bakhti and Y. Farzan, *JHEP* **07**, 064 (2014), [arXiv:1403.0744 \[hep-ph\]](#).
- [75] I. Mocioiu and W. Wright, *Nucl. Phys.* **B893**, 376 (2015), [arXiv:1410.6193 \[hep-ph\]](#).
- [76] P. Coloma, M. C. Gonzalez-Garcia, M. Maltoni, and T. Schwetz, (2017), [arXiv:1708.02899 \[hep-ph\]](#).
- [77] J. Liao and D. Marfatia, (2017), [arXiv:1708.04255 \[hep-ph\]](#).
- [78] I. Esteban, M. C. Gonzalez-Garcia, M. Maltoni, I. Martinez-Soler, and J. Salvado, *JHEP* **08**, 180 (2018), [arXiv:1805.04530 \[hep-ph\]](#).
- [79] K. Abe *et al.* (T2K), *PTEP* **2015**, 043C01 (2015), [arXiv:1409.7469 \[hep-ex\]](#).
- [80] S. B. Kim, (2000), talk given the KOSEF-JSPS Joint Seminar on New Developments in Neutrino Physics, Korea Institute for Advanced Study, Seoul, 2000.
- [81] K. Hagiwara, *Neutrino mass and seesaw mechanism. Proceedings, Fujihara Seminar, Tsukuba, Japan, February 23-25, 2004*, *Nucl. Phys. Proc. Suppl.* **137**, 84 (2004), [arXiv:hep-ph/0410229 \[hep-ph\]](#).
- [82] M. Ishitsuka, T. Kajita, H. Minakata, and H. Nunokawa, *Phys. Rev.* **D72**, 033003 (2005), [hep-ph/0504026](#).
- [83] K. Hagiwara, N. Okamura, and K.-i. Senda, *Phys. Lett.* **B637**, 266 (2006), [hep-ph/0504061](#).
- [84] K. Hagiwara, N. Okamura, and K.-i. Senda, *Phys. Rev.* **D76**, 093002 (2007), [arXiv:hep-ph/0607255](#).
- [85] T. Kajita, H. Minakata, S. Nakayama, and H. Nunokawa, *Phys. Rev.* **D75**, 013006 (2007), [hep-ph/0609286](#).
- [86] V. Barger, P. Huber, D. Marfatia, and W. Winter, *Phys. Rev. D* **76**, 053005 (2007), [arXiv:0703029 \[hep-ph\]](#).
- [87] K. Kimura, A. Takamura, and T. Yoshikawa, *JHEP* **03**, 016 (2008), [arXiv:0711.1567 \[hep-ph\]](#).
- [88] N. C. Ribeiro *et al.*, (2007), [arXiv:0712.4314 \[hep-ph\]](#).
- [89] P. Huber, M. Mezzetto, and T. Schwetz, *JHEP* **03**, 021 (2008), [arXiv:0711.2950 \[hep-ph\]](#).
- [90] K. Hagiwara and N. Okamura, *JHEP* **07**, 031 (2009), [arXiv:0901.1517 \[hep-ph\]](#).
- [91] H. Oki and O. Yasuda, *Phys. Rev.* **D82**, 073009 (2010), [arXiv:1003.5554 \[hep-ph\]](#).

- [92] K. Hagiwara, N. Okamura, and K.-i. Senda, *JHEP* **09**, 082 (2011), [arXiv:1107.5857 \[hep-ph\]](#).
- [93] K. Hagiwara, T. Kiwanami, N. Okamura, and K.-i. Senda, *JHEP* **06**, 036 (2013), [arXiv:1209.2763 \[hep-ph\]](#).
- [94] F. Dufour, (2012), [arXiv:1211.3884 \[hep-ph\]](#).
- [95] K. Hagiwara, P. Ko, N. Okamura, and Y. Takaesu, (2016), [arXiv:1605.02368 \[hep-ph\]](#).
- [96] P. Huber, M. Lindner, and W. Winter, *Comput. Phys. Commun.* **167**, 195 (2005), [hep-ph/0407333](#).
- [97] P. Huber, J. Kopp, M. Lindner, M. Rolinec, and W. Winter, *Comput. Phys. Commun.* **177**, 432 (2007), [hep-ph/0701187](#).
- [98] M. Blennow and E. Fernandez-Martinez, *Comput. Phys. Commun.* **181**, 227 (2010), [arXiv:0903.3985 \[hep-ph\]](#).
- [99] S. Fukasawa, (2017), ph.D. thesis, http://musashi.phys.se.tmu.ac.jp/theses/s_fukasawa_dt.pdf.
- [100] R. Foot, R. R. Volkas, and O. Yasuda, *Phys. Rev.* **D58**, 013006 (1998), [arXiv:hep-ph/9801431 \[hep-ph\]](#).
- [101] O. Yasuda, *Phys. Rev.* **D58**, 091301 (1998), [arXiv:hep-ph/9804400 \[hep-ph\]](#).
- [102] O. Yasuda, (2000), [arXiv:hep-ph/0006319 \[hep-ph\]](#).
- [103] S. Fukasawa and O. Yasuda, *Adv. High Energy Phys.* **2015**, 820941 (2015), [arXiv:1503.08056 \[hep-ph\]](#).